Title

Soluble adenylyl cyclase is an acid-base sensor in epithelial base-secreting cells

Journal

American Journal of Physiology - Cell Physiology, 311(2)

ISSN

0363-6143

Authors

Roa, Jinae N

Tresguerres, Martin

Publication Date

2016-08-01

DOI

10.1152/ajpcell.00089.2016

Peer reviewed

Soluble adenylyl cyclase is an acid-base sensor in epithelial base-secreting cells

Jinae N. Roa and Martin Tresguerres

Am J Physiol Cell Physiol 311:C340-C349, 2016. First published 22 June 2016;
doi: 10.1152/ajpcell.00089.2016

Am J Physiol Cell Physiol 311: C340–C349, 2016.
First published June 22, 2016; doi:10.1152/ajpcell.00089.2016.

Soluble adenylyl cyclase is an acid-base sensor in epithelial base-secreting cells

Jinae N. Roa and Martin Tresguerres

Marine Biology Research Division, Scripps Institution of Oceanography, University of California San Diego, La Jolla, California

Submitted 31 March 2016; accepted in final form 16 June 2016

Roa JN, Tresguerres M. Soluble adenylyl cyclase is an acid-base sensor in epithelial base-secreting cells. *Am J Physiol Cell Physiol* 311: C340–C349, 2016. First published June 22, 2016; doi:10.1152/ajpcell.00089.2016.—Blood acid-base regulation by specialized epithelia, such as gills and kidney, requires the ability to sense blood acid-base status. Here, we developed primary cultures of ray (*Urolophus halleri*) gill cells to study mechanisms for acid-base sensing without the interference of whole animal hormonal regulation. Ray gills have abundant base-secreting cells, identified by their noticeable expression of vacuolar-type H^+-ATPase (VHA), and also express the evolutionarily conserved acid-base sensor soluble adenylyl cyclase (sAC). Exposure of cultured cells to extracellular alkalosis (pH 8.0, 40 mM HCO_3^-) triggered VHA translocation to the cell membrane, similar to previous reports in live animals experiencing blood alkalosis. VHA translocation was dependent on sAC, as it was blocked by the sAC-specific inhibitor KH7. Ray gill base-secreting cells also express transmembrane adenylyl cyclases (tmACs); however, tmAC inhibition by 2′,5′-dideoxyadenosine did not prevent alkalosis-dependent VHA translocation, and tmAC activation by forskolin reduced the abundance of VHA at the cell membrane. This study demonstrates that sAC is a necessary and sufficient sensor of extracellular alkalosis in ray gill base-secreting cells. In addition, this study indicates that different sources of cAMP differentially modulate cell biology.

soluble adenylyl cyclase; pH sensing; proton pump; cAMP; gill

REGULATION OF SYSTEMIC acid-base status is essential for animal homeostasis. Vertebrates developed specialized epithelia that transport H^+, HCO_3^-, and other acid-base-relevant ions between the blood and the external environment, thus maintaining a stable internal milieu (14, 20, 35). For example, specialized cells in kidney and gill epithelia either secrete H^+ and absorb HCO_3^- to correct blood acidosis or secrete HCO_3^- and absorb H^+ to correct blood alkalosis (13, 47). Regulation and coordination of H^+ and HCO_3^- secretion and absorption rely on the ability of these cells to sense blood acid-base status; however, the molecular and cellular sensing mechanisms are largely unknown. Soluble adenylyl cyclase (sAC, adcy10) is one of the few evolutionarily conserved acid-base sensors identified to date (7, 10). Like the traditional transmembrane adenylyl cyclases (tmACs, adcy1-9), sAC produces cAMP and, therefore, can potentially modulate multiple aspects of cell biology via PKA-dependent phosphorylation, exchange protein regulated by cAMP, and cyclic nucleotide-gated channels (42). However, unlike tmACs, which are modulated by hormonal/G protein-coupled receptor (GPCR) pathways, sAC activity is, instead, directly responsive to CO_2, pH, and HCO_3^- levels (38). The fact that sAC and tmACs can coexist in the same cell raises the following question: How can the same messenger molecule, in this case cAMP, modulate multiple aspects of cell biology in a coordinated fashion? A potential explanation involves "cAMP microdomains," each with a distinct source of cAMP and phosphodiesterases that restrict cross-communication of cAMP from the different sources (reviewed in Refs. 11 and 42).

In α-intercalated cells (α-ICs) of the mammalian kidney distal tubule, sAC colocalizes with vacuolar-type H^+-ATPase (VHA) at the apical pole (14, 20, 26, 35). In isolated α-ICs, cell-permeable cAMP induced insertion of VHA into the apical membrane, as well as elongation of microvilli and upregulation of H^+ secretion (13, 27, 47), and in α-ICs from kidney slices, addition of the sAC-specific inhibitor KH7 reduced VHA insertion into the apical membrane (7, 10, 15). However, a direct relationship between acid-base sensing by sAC and apical VHA accumulation has yet to be established in α-ICs, in part because α-ICs are relatively scarce and difficult to identify in culture and because isolated α-ICs, as well as kidney slices, cannot withstand experimental acid-base conditions that deviate from ideal (pH 7.4, ~25 mM HCO_3^-, 5% CO_2) (5, 15, 42). However, research on clear cells of the mammalian epididymis has advanced our mechanistic understanding about acid-base sensing and H^+ secretion in renal α-ICs, because they are functionally and embryologically similar (19, 38), and, unlike renal tubules, they can be isolated and perfused with saline solutions with a wide pH and HCO_3^- concentration range (11, 25, 42). In clear cells, sensing of luminal alkalization by sAC and subsequent cAMP production trigger the insertion of VHA into the apical membrane and H^+ secretion into the lumen, a process used to maintain the acidic luminal pH required to maintain sperm in the quiescent state (25).

The mammalian distal tubule also regulates systemic acid-base status with β-intercalated cells (β-ICs), which secrete HCO_3^- in exchange for luminal Cl^- via apical pendrin anion exchangers (31) and absorb H^+ via basolateral VHA (6). sAC colocalizes with pendrin at the apical pole of β-ICs and with VHA near the basolateral membrane (26), suggesting that sAC senses the acid-base status and regulates the activity of pendrin and VHA accordingly; however, functional studies on acid-base sensing and regulation in β-ICs are scarce. The base-secreting cells in the gill of elasmobranch fishes (e.g., sharks, skates, and rays) provide a great surrogate model to β-ICs, as they also express VHA (28, 39), pendrin (28, 30), and sAC (44). These cells can simply be referred to as "VHA-rich cells," because, unlike mammalian kidney cells, they are the only gill cells that express noticeable amounts of VHA (39). Furthermore, elasmobranchs experience pronounced postprandial

Address for reprint requests and other correspondence: M. Tresguerres, 9500 Gilman Dr., Mail Code 0202, La Jolla, CA 92093 (e-mail: mtresguerres@ucsd.edu).

blood alkalosis after feeding, whereby pH can increase by ~0.3 pH units and HCO_3^- concentration can more than double (from ~4 to >10 mM, depending on meal size) over 24 h (48–50). These characteristics are major advantages for inducing experimental alkalosis without compromising cell viability. Elasmobranchs provide two additional advantages for studies on acid-base sensing and regulation: *1*) unlike mammals, which use both lungs and kidneys for blood acid-base regulation, elasmobranchs exclusively rely on their gills to maintain blood acid-base homeostasis (17), and *2*) unlike the mammalian kidney and bony fish gills, elasmobranch gills transport ions only for acid-base purposes and are not involved in NaCl transport for salt and osmoregulation (for which elasmobranches use their unique rectal gland) (17). These two characteristics allow study of acid-base regulatory mechanisms without the interference of osmoregulation, thus facilitating interpretation of results.

Experiments with live sharks have provided abundant mechanistic information about acid-base sensing and regulation: sAC triggered the translocation of VHA from cytoplasmic vesicles into the basolateral membrane of VHA-rich cells in response to blood alkalosis (44) through a mechanism that also depends on carbonic anhydrases (CAs) (45) and functional microtubules (43). Blocking VHA translocation with pharmacological inhibitors of sAC, CA, and microtubule assembly prevented sharks from effectively regulating blood acid-base homeostasis, indicating that basolateral VHA absorbs H^+ into the blood and powers apical HCO_3^- into seawater to correct blood alkalosis (43–45). However, since those experiments were performed on live, whole animals, it is unclear if direct sensing by sAC is sufficient or if hormonal control also contributes to the acid-base-sensing mechanism of VHA-rich cells. However, this and other mechanistic aspects of acid-base sensing, signal transduction, and acid-base regulation can be studied only in cell cultures.

In this study we developed primary gill cell cultures from the Pacific round ray (*Urolophus halleri*) to study acid-base sensing by sAC in base-secreting VHA-rich cells. Similar to native elasmobranch gill epithelium (30), isolated VHA-rich cells had a large number of mitochondria and expressed both sAC and tmACs. Exposure of isolated gill cells to extracellular alkalosis led to VHA translocation from the cytoplasm to the cell membrane in a sAC-dependent manner, confirming sAC as a necessary acid-base sensor in base-secreting cells. Furthermore, the tmAC agonist forskolin induced removal of VHA from the cell membrane, supporting the presence of cAMP microdomains in ray gill base-secreting cells.

METHODS

Experimental animals. All experiments were approved by the Scripps Institute of Oceanography-University of California San Diego Animal Care Committee under protocol number S10320 in compliance with the Institutional Animal Care and Use Committee guidelines for the care and use of experimental animals. Round rays were caught from La Jolla Shores, CA, housed in tanks with flowing seawater, and fed chopped squid or mackerel three times a week. Gill samples for cell isolation experiments were collected 2–3 days after the animals were fed.

Gill tissue sampling. Specimens were euthanized by an overdose of tricaine methanesulfonate (0.5 g/l), and gill samples were taken for the different experimental procedures. For immunohistochemistry, gill samples were fixed in 0.2 M cacodylate buffer, 3.2% paraformaldehyde, and 0.3% glutaraldehyde for 6 h, transferred to 50% ethanol for 6 h, and stored in 70% ethanol until further processing, as described by Tresguerres et al. (39). For Western blot analysis, gill samples were flash-frozen in liquid nitrogen and stored at −80°C.

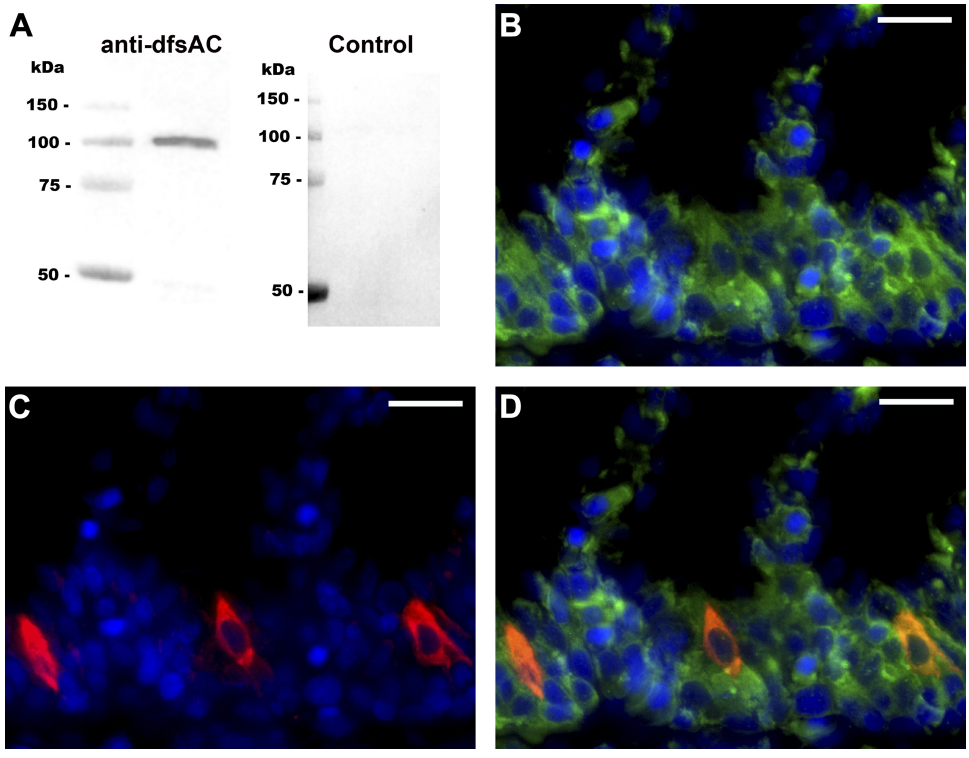

Fig. 1. Soluble adenylyl cyclase (sAC) in ray gills. *A*: anti-dogfish sAC (dfsAC) antibodies specifically recognized a 110-kDa shark sAC band in Western blots from gill crude homogenate, but not in peptide preabsorption control blots. *B–D*: sAC immunoreactivity was highly abundant in gill cells, with sAC (*B*, green) and vacuolar-type H^+-ATPase (VHA; *C*, red) immunoreactivity colocalized in VHA-rich base-secreting cells along the interlamellar gill region (*D*). Nuclei stained blue. Scale bars = 20 μm.

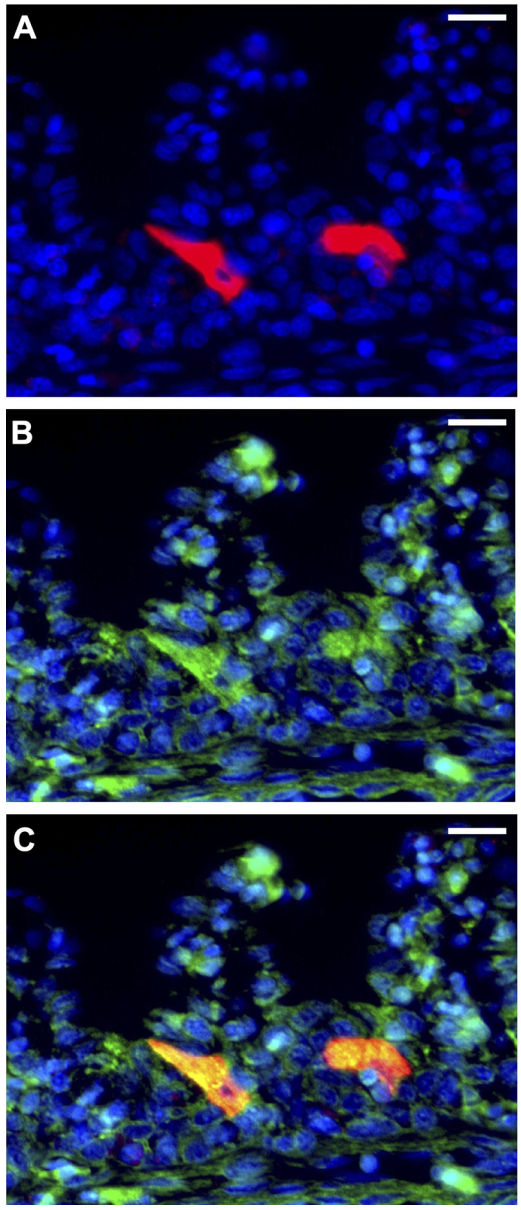

Fig. 2. Transmembrane adenylyl cyclases (tmACs) in vacuolar-type H^+-ATPase (VHA)-rich cells. *A–C*: VHA immunoreactivity (*A*, red) and BODIPY FL forskolin-labeled tmACs (*B*, green) are present together in cells along the interlamellar gill region (*C*). Nuclei stained blue. Scale bars = 20 μm.

Antibodies and reagents. Two custom-made polyclonal rabbit antibodies were used, one against a conserved peptide in the VHA B-subunit (30) (AREEVPGRRGFPGY) and the other against an epitope in the second catalytic domain of dogfish sAC (dfsAC) (44) (INNEFRNYQGRINKC). The anti-VHA antibodies specifically recognize the conserved VHA B-subunit in sharks (30, 44), corals (1), and marine worms (40). Another custom-made anti-VHA monoclonal mouse antibody against the same peptide was used to colocalize VHA and sAC on the same histological sections. BODIPY FL forskolin dye (Thermo Fisher Scientific, Waltham, MA) was used to determine tmAC localization [recently used to localize tmACs in mammalian cell cultures (8, 22) and zebrafish (21)], and MitoTracker Red (Thermo Fisher Scientific) was used to stain mitochondria in live cells. KH7 was a kind gift of Dr. Lonny Levin and Dr. Jochen Buck (Weill Cornell Medical College); forskolin and adenosine 3′,5′-cyclic monophosphorothioate (Sp-cAMP) were purchased from Enzo Life Sciences (Farmingdale, NY), and 2′,5′-dideoxyadenosine (DDA) was obtained from CalBiotech (Spring Valley, CA).

Western blotting. A procedure similar to that described by Roa et al. (30) was used to process frozen gill samples for Western blotting. Total protein (20 μg) was separated on a 7.5% polyacrylamide mini gel (60 V for 15 min, 200 V for 45 min) and transferred to a polyvinylidene difluoride (PVDF) membrane (Bio-Rad, Hercules, CA). After transfer, PVDF membranes were incubated in blocking buffer (Tris-buffered saline, 1% Tween, and 5% milk) at room temperature for 1 h and incubated in the primary antibody at 4°C overnight (3 μg/ml anti-dfsAC). PVDF membranes were washed three times and incubated in secondary antibody (1:10,000 dilution) at room temperature for 1 h. Bands were made visible through addition of ECL Prime Western blotting detection reagent (GE Healthcare, Waukesha, WI) and imaged and analyzed in a Bio-Rad Universal III hood using ImageQuant software (Bio-Rad). PVDF membranes incu-

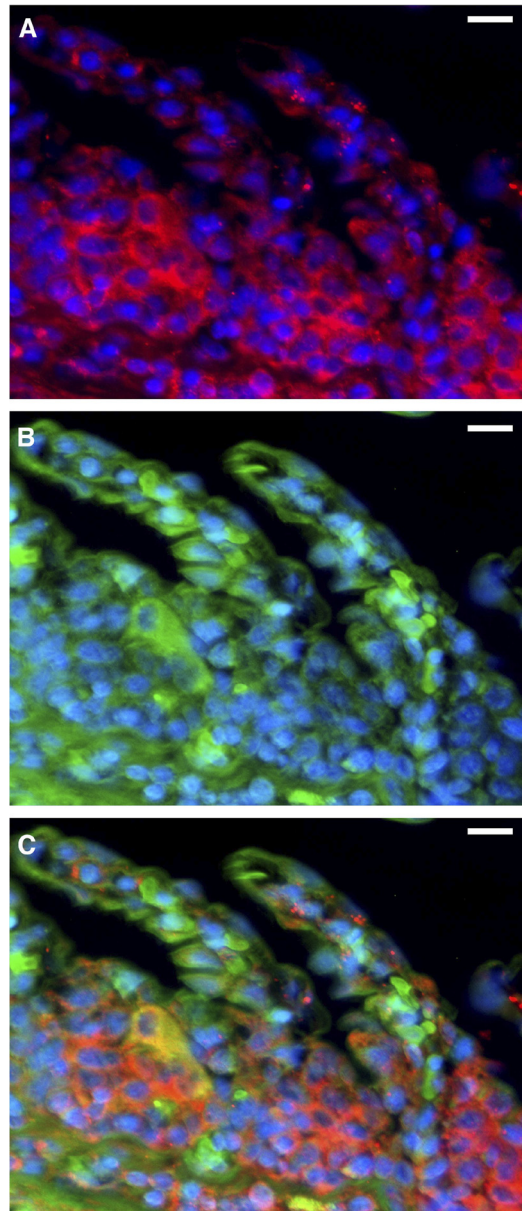

Fig. 3. Soluble adenylyl cyclase (sAC) and transmembrane adenylyl cyclases (tmACs) in ray gills. *A–C*: sAC immunoreactivity (*A*, red) and BODIPY FL forskolin-labeled tmACs (*B*, green) are present together in cells along the interlamellar gill region (*C*). Nuclei stained blue. Scale bars = 20 μm.

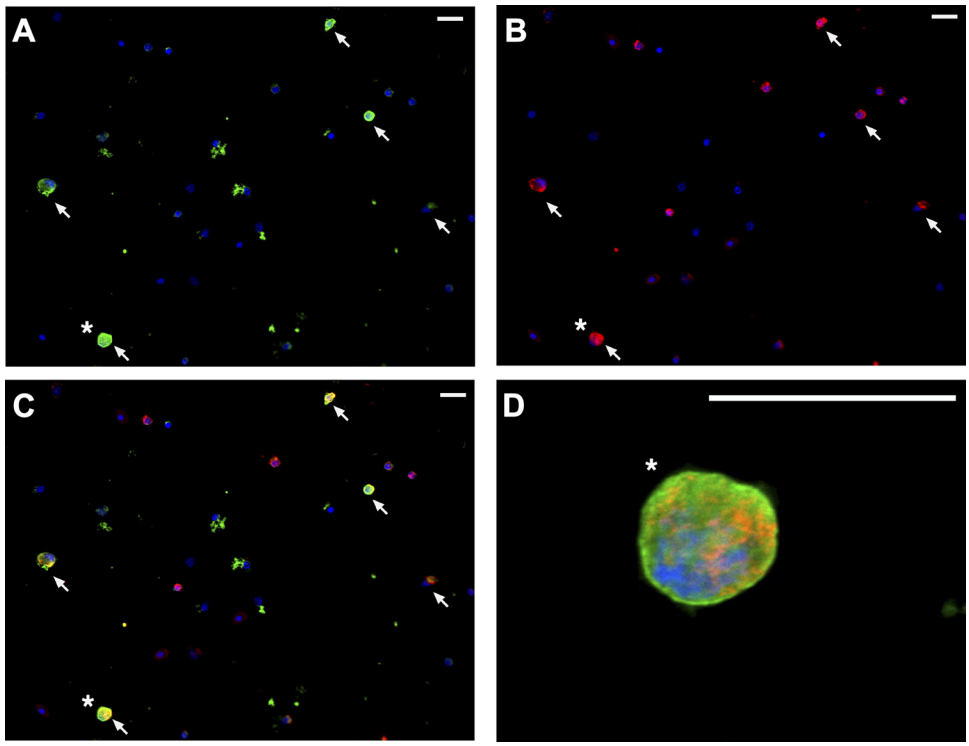

Fig. 4. Soluble adenylyl cyclase (sAC) in isolated gill cells. *A–C*: arrows indicate isolated mitochondrion-rich acid-base regulatory cells. sAC immunoreactivity was cytoplasmic (*A*, green), with viable mitochondrion-rich cells identified with MitoTracker Red (*B*, red), and merged image (*C*). *D*: higher magnification of the cell marked with an asterisk. Nuclei stained blue. Scale bars = 20 μm.

bated in blocking buffer with anti-dfsAC antibodies and threefold excess blocking peptide served as control and did not show any bands.

Immunohistochemistry. Gills fixed and stored in 70% ethanol as described above were processed using a procedure similar to that described by Roa et al. (30). Sections were blocked for 1 h (PBS, 2% normal goat serum, and 0.02% keyhole limpet hemocyanin, pH 7.7) and then incubated in the primary antibody overnight at 4°C (6 μg/ml anti-VHA, 12 μg/ml anti-dfsAC, and 10 μM BODIPY FL forskolin). Slides were washed three times in PBS, incubated in the appropriate secondary antibody (1:500 dilution) at room temperature for 1 h, incubated with the nuclear stain Hoechst 33342 (Invitrogen, Grand Island, NY; 5 μg/ml) for 5 min, washed three times in PBS, and permanently mounted in FluoroGel with Tris buffer (Electron Microscopy Sciences, Hatfield, PA). Immunofluorescence was detected using an epifluorescence microscope (Zeiss AxioObserver Z1) connected to a metal halide lamp and appropriate filters. Zeiss Axiovision software and Adobe Photoshop were used to adjust digital images for brightness and contrast only. Antigen retrieval was required for anti-dfsAC, which involved incubating slides in heated (95°C) citrate unmasking buffer (10 mM citric acid and 0.05% Tween 20, pH 6.0) for 30 min following rehydration. For anti-dfsAC, control sections incubated in blocking buffer with anti-dfsAC antibodies and 300-fold excess blocking peptide showed no visible sAC immunoreactivity.

Colocalization of sAC, VHA, and tmACs. For immunolocalization of sAC to VHA-rich cells, sections were processed as described above but incubated in a mixture of anti-dfsAC (rabbit) and anti-VHA (mouse) antibodies overnight and then in a mixture of goat anti-rabbit and anti-mouse secondary antibodies. Similarly, mixtures of BODIPY FL forskolin dye with anti-dfsAC or anti-VHA antibodies were used to colocalize tmACs with sAC or VHA, with sections incubated in BODIPY FL forskolin (30 min) and treated as described above.

Isolated gill cells. A collagenase digestion protocol used for isolating cells from trout gills (24) was optimized for ray gills. Gills were perfused through the heart with 50 ml of ice-cold heparinized shark saline (280 mM NaCl, 6 mM KCl, 5 mM $NaHCO_3$, 3 mM $MgCl_2$, 0.5 mM $NaSO_4$, 1 mM Na_2HPO_4, 350 mM urea, 70 mM trimethylamine *N*-oxide, 5 mM glucose, and 1:100 dilution of protease inhibitor

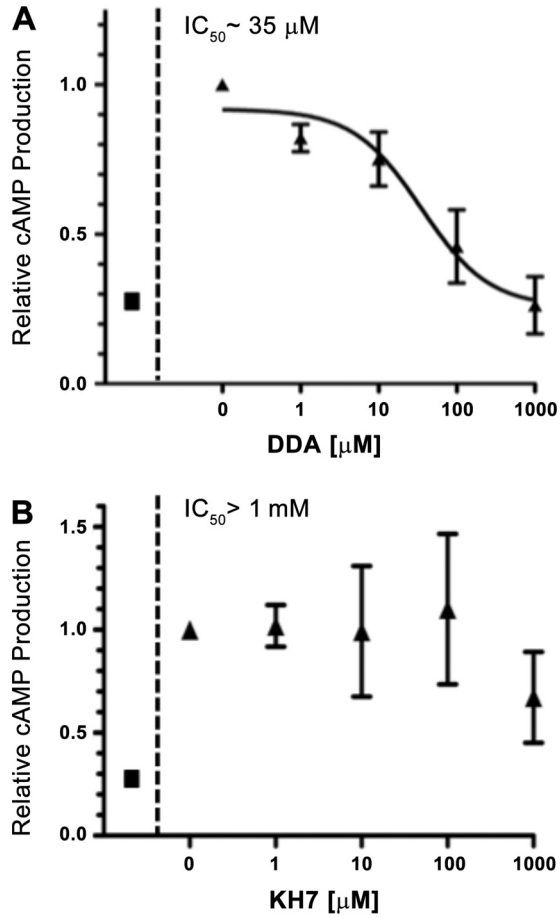

Fig. 5. Transmembrane adenylyl cyclase (tmAC) activity in ray gills. *A* and *B*: forskolin (10 μM) stimulated a 4-fold increase in cAMP over control cAMP concentrations (■), which was inhibited by low concentrations of 2′,5′-dideoxyadenosine (DDA, IC_{50} = 35 μM), but not KH7 (IC_{50} >1 mM).

cocktail, pH 7.7), and 5-mm-wide sections were dissected and incubated for 20 min (3 times) in a collagenase-saline solution (0.2 mg/ml). Cell suspensions were filtered onto a 50:50 FBS-saline solution to inactivate collagenase activity. Final cell suspensions were washed (3 times) with 10 ml of saline solution, centrifuged at 1,500 *g* (4°C), resuspended in 5 ml of saline solution, plated onto poly-L-lysine-coated coverslips, and allowed to settle for 2 h. After cells recovered, they were exposed to control saline (+DMSO), saline

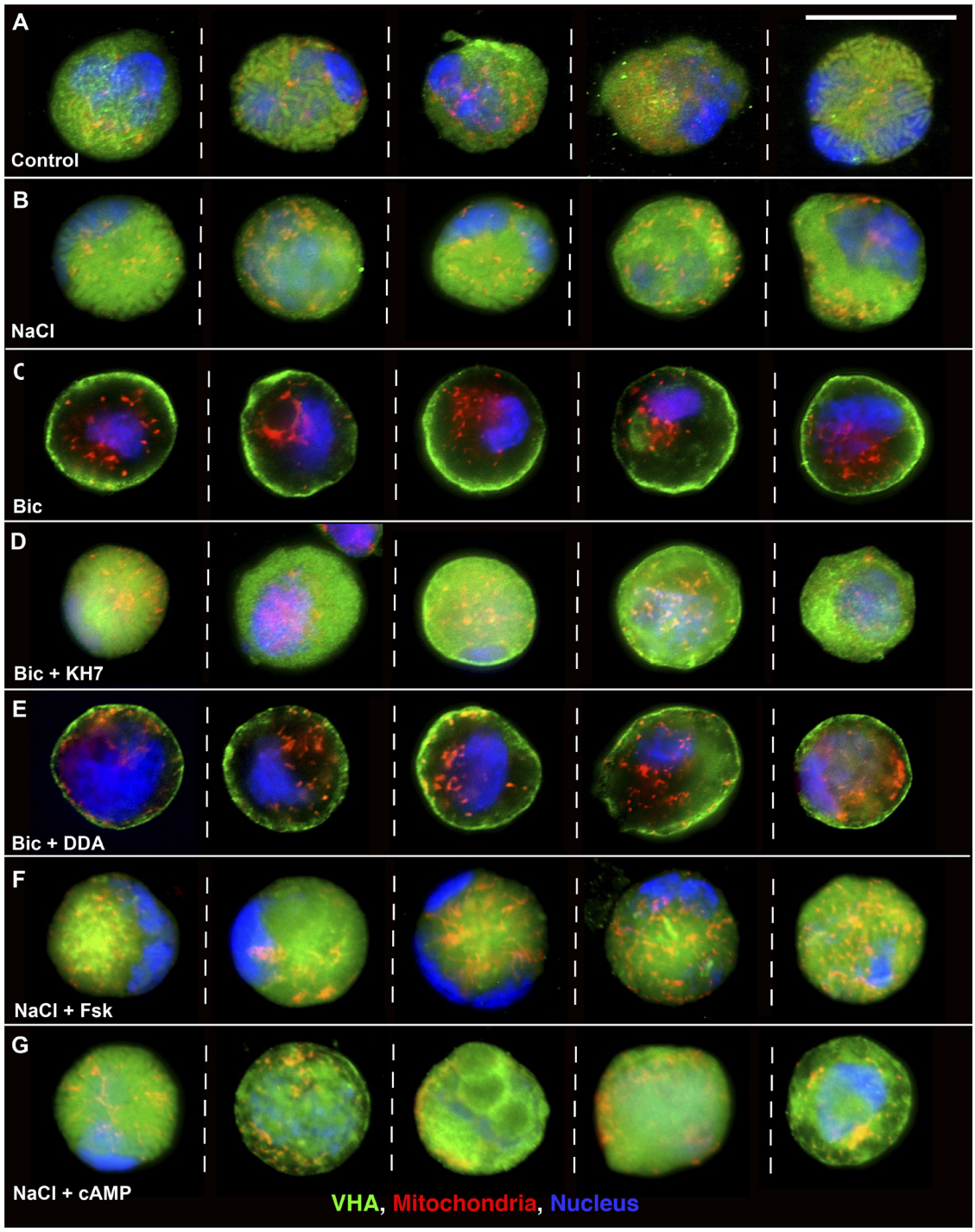

Fig. 6. Vacuolar-type H^+-ATPase (VHA) translocates to the cell membrane of isolated base-secreting cells exposed to extracellular alkalosis. Representative images of 5 separate cells (all cells from the same ray) show VHA (green) localization in isolated cells exposed to control (5 mM HCO_3^-, pH 7.75, $n = 59$), NaCl (5 mM HCO_3^- + 40 mM NaCl, pH 7.75, $n = 60$), Bic (40 mM HCO_3^-, pH 8.0, $n = 56$), Bic + KH7 (50 μM KH7 + 40 mM HCO_3^-, pH 8.0, $n = 60$), Bic + DDA (100 μM DDA + 40 mM HCO_3^-, pH 8.0, $n = 60$), NaCl + Fsk (10 μM forskolin + 5 mM HCO_3^- + 40 mM NaCl, pH 7.75, $n = 60$), and NaCl + cAMP (1 mM Sp-cAMP + 5 mM HCO_3^- + 40 mM NaCl, pH 7.75, $n = 40$). VHA was cytoplasmic in cells exposed to control (*A*) and NaCl (*B*); VHA translocated to the cell membrane in cells exposed to alkalosis (*C*, Bic). Alkalosis-induced VHA translocation was blocked by KH7 (*D*, Bic + KH7), but not by DDA (*E*, Bic + DDA). Additionally, VHA was cytoplasmic in cells exposed to forskolin (*F*, NaCl + Fsk) and Sp-cAMP (*G*, NaCl + cAMP). Nuclei stained blue; mitochondria stained red. Scale bars = 20 μm.

with additional 40 mM NaCl (320 mM NaCl + DMSO), NaCl saline + forskolin (10 μM forskolin in DMSO), NaCl saline + Sp-cAMP (1 mM Sp-cAMP in DMSO), saline with additional 40 mM $NaHCO_3$ (pH 8.0), and the latter saline with KH7 (50 μM KH7 in DMSO) or DDA (100 μM DDA in DMSO) for 30 min. Cells were then incubated in the active mitochondrial dye MitoTracker Red (200 nM, 30 min), fixed (shark saline, 3.2% paraformaldehyde, and 0.3% glutaraldehyde for 20 min), incubated in anti-VHA antibodies overnight, and processed for immunocytochemistry as described above. HCO_3^- and pH values of the incubation medium were confirmed using a CO_2 analyzer (Corning, Corning, NY) and UltraBASIC pH meter (Denver Instrument, Bohemia, NY).

cAMP assays. Tissue homogenates were incubated for 30 min at room temperature in an orbital shaker (300 rpm) in 100 mM Tris (pH 7.5), 5 mM ATP, 10 mM $MgCl_2$, 0.1 mM $MnCl_2$, 0.5 mM IBMX, 1 mM dithiothreitol, 20 mM creatine phosphate, and 100 U/ml creatine phosphokinase. For inhibition of tmAC activity, tissue homogenates were incubated in 10 μM forskolin and the indicated concentrations of KH7 and DDA. cAMP concentrations were determined using DetectX Direct Cyclic AMP Enzyme Immunoassay (Arbor Assays, Ann Arbor, MI).

Quantification of VHA translocation. VHA localization in response to each experimental treatment was determined in ~40–60 cells from two or three different rays. Starting from the upper-right corner of the field of view, the first ~20 VHA-positive cells with strong mitochondrial staining (30) were selected and individually imaged at ×600 magnification. The individual performing the imaging was not aware of the treatment that was being analyzed ("blind examiner"). Cells with distinct "ring" VHA immunostaining (strong signal in the cell membrane and lack of signal in the cytoplasm) were counted as cells with "membrane VHA localization," while cells without distinct membrane staining [cytoplasmic and intermediate staining (43, 44)] were grouped together as non-membrane-staining. Additionally, fluorescence intensity was quantified across the length of the cell using ImageJ analysis software. Fluorescence intensity histograms were created by drawing transects across individual cells while avoiding the nuclei. To avoid bias, two transects per cell were used, and the data were averaged. Data were normalized for cell size and background fluorescence, and then (above-average) fluorescence at the edge of the cell (first and last 10%) was quantified and divided by (above-average) total cell fluorescence to give "relative VHA membrane abundance" or VHA abundance from the edge to the center of each cell. This analysis was performed using a custom-made script written in Python programming language, into which images were input randomly to eliminate bias.

Statistical analysis. Individual cells were counted as experimental replicates ($n = 40–60$ cells from 2–3 rays), similar to previous studies from mammalian kidney intercalated cells and epididymal clear cells (25, 27). All quantitative data were arcsine-transformed, and experimental groups were analyzed for significant differences using a one- or two-way ANOVA and Bonferroni's multiple-comparison test ($P < 0.001$).

RESULTS

sAC is present in ray VHA-rich cells, alongside tmACs. Antibodies against dfsAC (anti-dfsAC) detected the predicted 110-kDa band for shark sAC in Western blots from ray gill extracts, but not in control blots (Fig. 1*A*). sAC immunofluorescence was present throughout the cytoplasm of gill cells in histological sections (Fig. 1*B*), and double immunolabeling with antibodies against VHA (Fig. 1*C*) also revealed high sAC abundance in base-secreting VHA-rich cells (Fig. 1*D*). Similar to results from previous studies of starved sharks (30, 39, 43–45), VHA was localized in the cytoplasm of starved ray gill cells. In addition, VHA-rich cells were labeled with BODIPY FL forskolin (Fig. 2), demonstrating that these cells express two distinct sources of cAMP: tmACs and sAC. In fact, sAC and tmACs colocalized in most cells throughout the ray gill epithelium (Fig. 3). As seen in histological gill sections, sAC was also present throughout the cytoplasm of gill isolated cells, including acid-base regulatory cells [identified by their abundant mitochondria (30), which were stained using the mitochondrial dye MitoTracker Red] (Fig. 4).

sAC inhibitor does not inhibit tmACs. In mammals, two types of adenylyl cyclases produce cAMP: tmACs, which are activated by hormones and GPCRs, and sAC. The only known pharmacological adenylyl cyclase activators are derivatives of forskolin, a natural plant dipentene that selectively binds tmACs, but not sAC (7, 34). DDA and KH7 are pharmacological inhibitors: DDA is tmAC-selective ($IC_{50} = 8$ μM) (3, 12), and the small molecule KH7 is sAC-selective ($IC_{50} = 10$ μM) (18). Tresguerres et al. (44) reported HCO_3^--stimulated, KH7-sensitive cAMP production in elasmobranch gill homogenates, as well as in purified elasmobranch sAC (EC_{50} $HCO_3^- = 5$ mM, IC_{50} KH7 = 10 μM). However, they did not test the effects of KH7 on elasmobranch tmACs. Therefore, we used forskolin-stimulated cAMP production to determine the inhibitory effects of DDA and KH7 on tmAC activity. Forskolin initiated a fourfold increase in cAMP activity (Fig. 5), an indication that tmACs are present and responsive to traditional forskolin-stimulated activation. DDA inhibited forskolin-stimulated tmAC activity ($IC_{50} = 35$ μM; Fig. 5*A*), and KH7 did not ($IC_{50} > 1$ mM; Fig. 5*B*), thereby validating the use of DDA and KH7 in subsequent tmAC- and sAC-inhibitory experiments.

sAC-dependent VHA translocation to the cell membrane. In VHA-rich cells exposed to control saline (control: 5 mM HCO_3^-, pH 7.75) and high-NaCl saline (NaCl: 5 mM HCO_3^- +

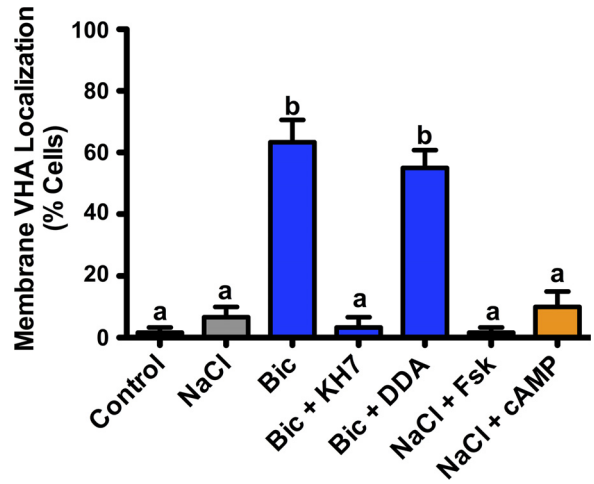

Fig. 7. sAC-dependent membrane vacuolar-type H^+-ATPase (VHA) localization in isolated base-secreting cells. Cells were exposed to control (5 mM HCO_3^-, pH 7.75, $n = 59$), NaCl (5 mM HCO_3^- + 40 mM NaCl, pH 7.75, $n = 60$), Bic (40 mM HCO_3^-, pH 8.0, $n = 56$), Bic + KH7 (50 μM KH7 + 40 mM HCO_3^-, pH 8.0, $n = 60$), Bic + DDA (100 μM DDA + 40 mM HCO_3^-, pH 8.0, $n = 60$), NaCl + Fsk (10 μM forskolin + 5 mM HCO_3^- + 40 mM NaCl, pH 7.75, $n = 60$), and NaCl + cAMP (1 mM Sp-cAMP + 5 mM HCO_3^- + 40 mM NaCl, pH 7.75, $n = 40$). 40 mM HCO_3^- ("Bic") significantly increased the percentage of cells with membrane VHA localization, which was inhibited by KH7, but not DDA ($P < 0.001$). Compared with control and NaCl cells, forskolin and Sp-cAMP had no effect on the percentage of cells with membrane VHA localization.

40 mM NaCl, pH 7.75), VHA was predominantly localized in the cytoplasm (Fig. 6, *A* and *B*). In cells exposed to alkaline, high-bicarbonate saline (Bic: 40 mM HCO_3^-, pH 8.0), VHA translocated to the cell membrane (Fig. 6*C*), which was similar to previous reports from live animals experiencing blood alkalosis (30, 39, 44). This alkalosis-induced VHA translocation was dependent on sAC, and not tmACs; VHA remained in the cytoplasm of cells exposed to the sAC-selective inhibitor KH7 (Bic + KH7; Fig. 6*D*) but translocated to the cell membrane of cells exposed to the tmAC-selective inhibitor DDA (Bic + DDA; Fig. 6*E*). Additionally, VHA was localized in the cytoplasm of cells exposed to the tmAC activator forskolin (NaCl + Fsk; Fig. 6*F*) and Sp-cAMP (NaCl + cAMP; Fig. 6*G*). Overall, the percentage of all cells with membrane VHA was significantly higher in cells exposed to alkaline saline, with or without DDA (Fig. 7). Furthermore, since VHA was cytoplasmic in cells exposed to high-NaCl saline, alkalosis, rather than increased ionic strength and osmolarity, is the trigger of VHA translocation.

An additional analysis of VHA translocation based on the histogram of fluorescence intensity across the length of each cell yielded identical results (see METHODS for details). VHA fluorescence intensity in control cells and cells exposed to NaCl, Bic + KH7, NaCl + Fsk, and NaCl + cAMP was higher in the cytoplasmic center; in cells exposed to Bic and Bic + DDA, it peaked at the membrane edge (Fig. 8), with significantly higher relative VHA abundance at the membrane (0–10% from the cell edge) and lower relative VHA abundance in the cytoplasm (40–50% from the cell edge; Fig. 9). Since KH7, but not DDA, prevented alkalosis-induced VHA translocation, we conclude that sAC in each isolated VHA-rich cell is the molecular sensor of alkalosis that initiates an acid-base regulatory response, as previously suggested by experiments in live sharks (44).

tmAC-dependent VHA movement away from the cell membrane. Since ray gill VHA-rich cells also express tmACs, we examined the effect of forskolin on VHA translocation. Our hypothesis was that if cAMP produced by tmAC had the same

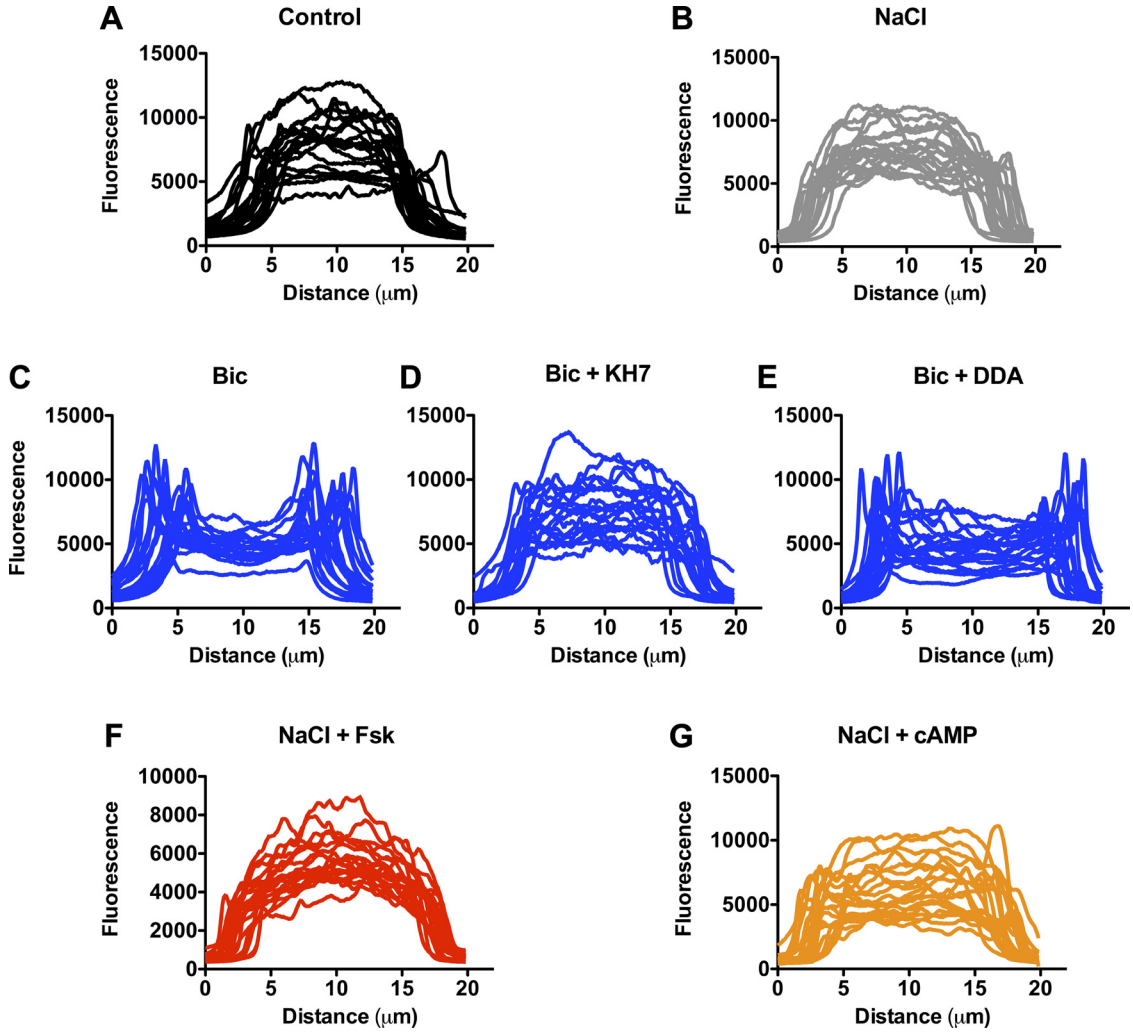

Fig. 8. Vacuolar-type H^+-ATPase (VHA) fluorescence intensity in isolated base-secreting cells. *A–G*: representative transects displaying VHA fluorescence intensity (created with ImageJ analysis software) of cells exposed to control (5 mM HCO_3^-, pH 7.75, $n = 59$), NaCl (5 mM HCO_3^- + 40 mM NaCl, pH 7.75, $n = 60$), Bic (40 mM HCO_3^-, pH 8.0, $n = 56$), Bic + KH7 (50 μM KH7 + 40 mM HCO_3^-, pH 8.0, $n = 60$), Bic + DDA (100 μM DDA + 40 mM HCO_3^-, pH 8.0, $n = 60$), NaCl + Fsk (10 μM forskolin + 5 mM HCO_3^- + 40 mM NaCl, pH 7.75, $n = 60$), and NaCl + cAMP (1 mM Sp-cAMP + 5 mM HCO_3^- + 40 mM NaCl, pH 7.75, $n = 40$).

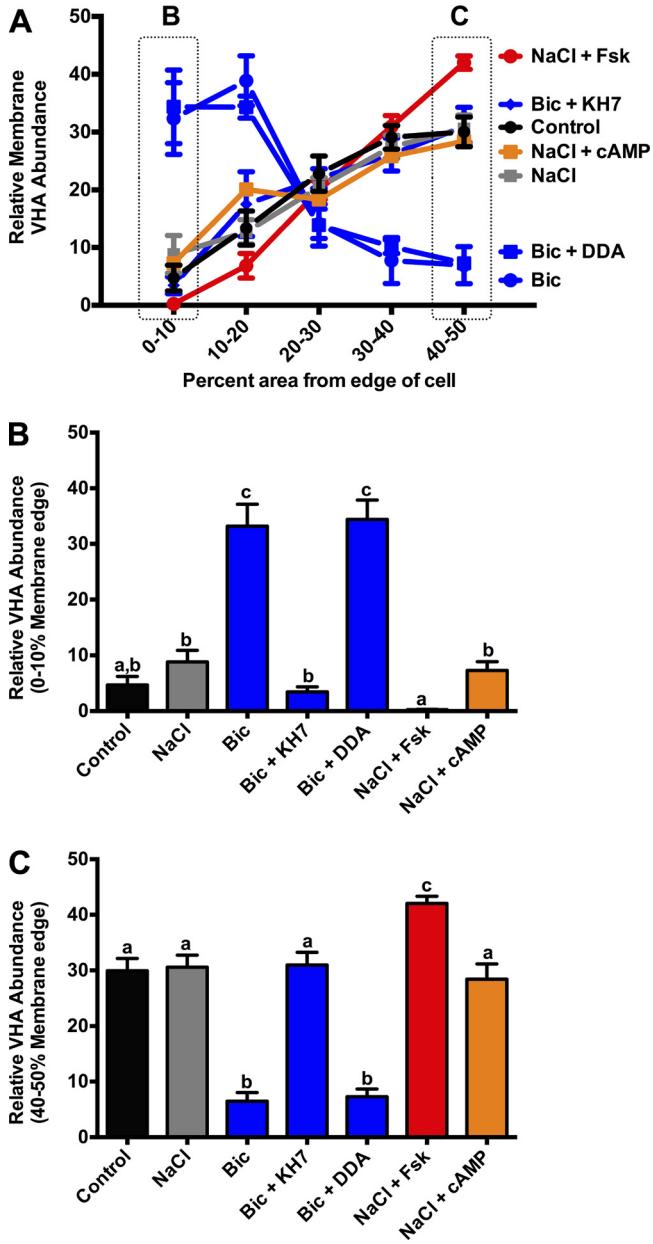

Fig. 9. Relative membrane vacuolar-type H^+-ATPase (VHA) abundance increased during extracellular alkalosis in isolated base-secreting cells. *A*: relative VHA abundance across cells exposed to control (5 mM HCO_3^-, pH 7.75, $n = 59$), NaCl (5 mM HCO_3^- + 40 mM NaCl, pH 7.75, $n = 60$), Bic (40 mM HCO_3^-, pH 8.0, $n = 56$), Bic + KH7 (50 μM KH7 + 40 mM HCO_3^-, pH 8.0, $n = 60$), Bic + DDA (100 μM DDA + 40 mM HCO_3^-, pH 8.0, $n = 60$), NaCl + Fsk (10 μM forskolin + 5 mM HCO_3^- + 40 mM NaCl, pH 7.75, $n = 60$), and NaCl + cAMP (1 mM Sp-cAMP + 5 mM HCO_3^- + 40 mM NaCl, pH 7.75, $n = 40$). *B*: 40 mM HCO_3^- ("Bic") significantly increased relative VHA abundance at the cell membrane (0–10% of the area from the edge of the cell), which was inhibited by KH7, but not DDA ($P < 0.001$). Compared with control and NaCl cells, forskolin and Sp-cAMP had no effect on relative membrane VHA abundance. *C*: 40 mM HCO_3^- ("Bic") significantly decreased relative VHA abundance in the cell cytoplasmic center (40–50% of the area from the edge of the cell), which was inhibited by KH7, but not DDA ($P < 0.001$). Compared with control and NaCl cells, forskolin significantly increased relative VHA abundance in the cell cytoplasmic center ($P < 0.001$), and Sp-cAMP had no effect.

effect as cAMP produced by sAC, VHA should translocate to the cell membrane, as observed during sAC stimulation by elevated bicarbonate. However, the effect of tmAC stimulation by forskolin is the opposite of the effect of stimulation by bicarbonate (Fig. 9*A*), as evidenced by less VHA at the cell membrane (Fig. 9*B*) and more VHA toward the center of the cell (Fig. 9*C*) than in the NaCl control cell. Addition of cell-permeable cAMP under control conditions had no effect on VHA translocation (Fig. 9), which is consistent with different pools of cAMP having opposing effects on VHA translocation, with no net effect.

DISCUSSION

Similar to previous studies on live sharks, exposure of isolated ray gill cells to alkaline conditions induced the translocation of VHA from the cytoplasm to the cell membrane, a process that was prevented by the sAC inhibitor KH7, but not by the tmAC inhibitor DDA. Thus, sAC in each VHA-rich cell is necessary and sufficient to sense alkalosis and trigger a compensatory response, as our experiments with isolated cultured cells rule out whole animal endocrine and paracrine signaling.

The results from this study, along with those from live elasmobranchs experiencing natural postfeeding (30, 45) and experimentally induced (39, 43, 44) blood alkalosis, yield the following model for sensing and counteracting blood alkalosis: elevated plasma HCO_3^- is dehydrated into CO_2 catalyzed by extracellular CA, which then diffuses inside gill VHA-rich cells and is hydrated back into H^+ and HCO_3^- by intracellular CA. The subsequent elevation of intracellular HCO_3^- stimulates sAC, which mediates, possibly via PKA-dependent phosphorylation of motor proteins, the microtubule-dependent translocation of VHA-containing vesicles from the cytoplasm to the basolateral membrane. The anion exchanger pendrin also translocates to the apical membrane in response to blood alkalosis (30); however, it is unknown whether this process is sAC-dependent. Basolateral VHA absorbs H^+ into the blood, and pendrin excretes HCO_3^- into seawater in exchange for Cl^-. H^+ absorbed by VHA combines with plasma HCO_3^-, generating more CO_2, and the process continues until plasma HCO_3^- returns to basal levels. The fact that VHA translocation still takes place in isolated and cultured gill VHA-rich cells demonstrates that this process is self-regulatory and self-sufficient. In addition to VHA-rich cells, sAC was present throughout the cytoplasm of other gill cells, suggesting that sAC regulates multiple other physiological processes. For example, sAC might regulate H^+ secretion and HCO_3^- absorption in acid-secreting Na^+-K^+-ATPase-rich cells, as well as the reversible hydration of CO_2 in pillar cells, as previously suggested (44). The ray gill cell cultures optimized in this study will be a valuable tool for the study of these and other elements of acid-base sensing and regulation.

Previous research has suggested a link between acid-base sensing by sAC and pH regulation by VHA in mammalian kidney β-ICs: metabolic alkalosis increased VHA abundance in basolateral membranes (32), and sAC colocalized with VHA at the basolateral region (26). However, functional studies on renal β-ICs are not available, probably because of their low abundance in the mammalian nephron, limited cell cultures, and their inability to tolerate exposure to highly alkaline

conditions in vivo without compromise to their viability. The cultured ray gill cells developed here circumvent these limitations, making them a promising surrogate model system for renal β-ICs. Furthermore, this acid-base-sensing and regulation model may apply to other epithelia known to have basolateral VHA-, sAC-, and cAMP-stimulated base secretion, but in which their potential link has not been studied. Some examples include mammalian pancreatic (29, 36, 46) and salivary (33) ducts, marine bony fish intestine (9, 16, 41), and insect midgut (4).

Staining with BODIPY FL forskolin suggested that, in addition to sAC, most ray gill cells express tmACs. This was confirmed by the robust forskolin-stimulated cAMP production in ray gill extracts that was sensitive to the tmAC inhibitor DDA. Furthermore, colocalization of VHA with sAC (using dual immunostaining) and with tmACs (using BODIPY FL forskolin staining) demonstrated the presence of both sAC and tmACs in VHA-rich cells. This situation also resembles the mammalian renal collecting duct, where α- and β-ICs are located, because it also expresses sAC (adcy10) (25, 26) and the tmACs (adcys2, adcys4, adcys5, adcys6, and adcys9) (2). However, DDA did not affect alkalosis-induced VHA translocation in cultured gill VHA-rich cells, and forskolin induced a redistribution of VHA away from the cell membrane. These results rule out a role of tmACs in triggering the VHA translocation and raise questions about the physiological roles of tmACs in these cells. Since tmAC stimulation induced an effect on VHA translocation that was the opposite of the effect of sAC, it is possible that tmACs are involved in the sensing of acidosis. For example, in mammalian renal collecting duct cells, tmACs are stimulated in response to extracellular metabolic acidosis through a mechanism that depends on the GPCR GPR4 (23, 37). We hypothesize that acid-base sensing and regulation in gill cells occur as a result of the coordinated action of sAC (which stimulates base secretion and inhibits acid secretion under alkalosis) and GPCR/tmAC (which stimulates acid secretion and inhibits base secretion under acidosis). Confirmation of this model will require, first, establishing whether any acid-sensing GPCRs are present in gill acid- and base-secreting cells. However, the subsequent experimental testing will not be trivial, because both sensing mechanisms depend on the same messenger molecule, cAMP, which complicates interpretation of results from experiments using cAMP agonists and antagonists.

In summary, this study established sAC as a sensor of alkalosis in ray gill base-secreting cells. Because sAC, the cAMP pathway, and VHA are widespread in eukaryotic cells, this could be an evolutionarily conserved mechanism for sensing and counteracting alkalosis.

ACKNOWLEDGMENTS

The authors are grateful to Phil Zerofski (Scripps Institute of Oceanography) for excellent assistance with experimental animal capture and husbandry and general aquarium matters.

GRANTS

J. N. Roa is supported by the William Townsend Porter Predoctoral Fellowship from the American Physiological Society. M. Tresguerres is supported by National Science Foundation Grant IOS 1354181 and Alfred P. Sloan Research Fellowship BR2013-103.

DISCLOSURES

No conflicts of interest, financial or otherwise, are declared by the authors.

AUTHOR CONTRIBUTIONS

J.N.R. and M.T. developed the concept and designed the research; J.N.R. performed the experiments; J.N.R. and M.T. analyzed the data; J.N.R. and M.T. interpreted the results of the experiments; J.N.R. prepared the figures; J.N.R. and M.T. drafted the manuscript; J.N.R. and M.T. edited and revised the manuscript; J.N.R. and M.T. approved the final version of the manuscript.

REFERENCES

1. **Barott KL, Venn AA, Perez SO, Tambutté S, Tresguerres M.** Coral host cells acidify symbiotic algal microenvironment to promote photosynthesis. *Proc Natl Acad Sci USA* 112: 607–612, 2015.
2. **Bek MJ, Zheng S, Xu J, Yamaguchi I, Asico LD, Sun XG, Jose PA.** Differential expression of adenylyl cyclases in the rat nephron. *Kidney Int* 60: 890–899, 2001.
3. **Bitterman JL, Ramos-Espiritu L, Diaz A, Levin LR, Buck J.** Pharmacological distinction between soluble and transmembrane adenylyl cyclases. *J Pharmacol Exp Ther* 347: 589–598, 2013.
4. **Boudko DY, Moroz LL, Harvey WR, Linser PJ.** Alkalinization by chloride/bicarbonate pathway in larval mosquito midgut. *Proc Natl Acad Sci USA* 98: 15354–15359, 2001.
5. **Breton S, Brown D.** Cold-induced microtubule disruption and relocalization of membrane proteins in kidney epithelial cells. *J Am Soc Nephrol* 9: 155–166, 1998.
6. **Brown D, Hirsch S, Gluck S.** An H^+-ATPase in opposite plasma membrane domains in kidney epithelial cell subpopulations. *Nature* 331: 622–624, 1988.
7. **Buck J, Sinclair ML, Schapal L, Cann MJ, Levin LR.** Cytosolic adenylyl cyclase defines a unique signaling molecule in mammals. *Proc Natl Acad Sci USA* 96: 79–84, 1999.
8. **Calebiro D, Nikolaev VO, Gagliani MC, de Filippis T, Dees C, Tacchetti C, Persani L, Lohse MJ.** Persistent cAMP-signals triggered by internalized G-protein-coupled receptors. *PLoS Biol* 7: e1000172, 2009.
9. **Carvalho ES, Gregório SF, Power DM, Canário AV, Fuentes J.** Water absorption and bicarbonate secretion in the intestine of the sea bream are regulated by transmembrane and soluble adenylyl cyclase stimulation. *J Comp Physiol B* 182: 1069–1080, 2012.
10. **Chen Y, Cann MJ, Litvin TN, Iourgenko V, Sinclair ML, Levin LR, Buck J.** Soluble adenylyl cyclase as an evolutionarily conserved bicarbonate sensor. *Science* 289: 625–628, 2000.
11. **Cooper DM.** Regulation and organization of adenylyl cyclases and cAMP. *Biochem J* 375: 517–529, 2003.
12. **Dessauer CW, Gilman AG.** The catalytic mechanism of mammalian adenylyl cyclase. Equilibrium binding and kinetic analysis of P-site inhibition. *J Biol Chem* 272: 27787–27795, 1997.
13. **Evans DH, Piermarini PM, Choe KP.** The multifunctional fish gill: dominant site of gas exchange, osmoregulation, acid-base regulation, and excretion of nitrogenous waste. *Physiol Rev* 85: 97–177, 2005.
14. **Frizzell RA, Field M, Schultz SG.** Sodium-coupled chloride transport by epithelial tissues. *Am J Physiol Renal Fluid Electrolyte Physiol* 236: F1–F8, 1979.
15. **Gong F, Alzamora R, Smolak C, Li H, Naveed S, Neumann D, Hallows KR, Pastor-Soler NM.** Vacuolar H^+-ATPase apical accumulation in kidney intercalated cells is regulated by PKA and AMP-activated protein kinase. *Am J Physiol Renal Physiol* 298: F1162–F1169, 2010.
16. **Guffey S, Esbaugh A, Grosell M.** Regulation of apical H^+-ATPase activity and intestinal HCO_3^- secretion in marine fish osmoregulation. *Am J Physiol Regul Integr Comp Physiol* 301: R1682–R1691, 2011.
17. **Heisler N.** Acid-base regulation. In: *Physiology of Elasmobranch Fishes*. Berlin: Springer, 1988, p. 215–252.
18. **Hess KC, Jones BH, Marquez B, Chen Y, Ord TS, Kamenetsky M, Miyamoto C, Zippin JH, Kopf GS, Suarez SS, Levin LR, Williams CJ, Buck J, Moss SB.** The "soluble" adenylyl cyclase in sperm mediates multiple signaling events required for fertilization. *Dev Cell* 9: 249–259, 2005.
19. **Hinton BT, Turner TT.** Is the epididymis a kidney analogue? *Physiology* 3: 28–31, 1988.
20. **Krogh A.** *Osmotic Regulation in Fresh Water Fishes by Active Absorption of Chloride Ions*. Copenhagen: University of Copenhagen, 1937.

21. **Kumai Y, Kwong RW, Perry SF.** The role of cAMP-mediated intracellular signaling in regulating Na^+ uptake in zebrafish larvae. *Am J Physiol Regul Integr Comp Physiol* 306: R51–R60, 2014.
22. **Kuna RS, Girada SB, Asalla S, Vallentyne J, Maddika S, Patterson JT, Smiley DL, DiMarchi RD, Mitra P.** Glucagon-like peptide-1 receptor-mediated endosomal cAMP generation promotes glucose-stimulated insulin secretion in pancreatic β-cells. *Am J Physiol Endocrinol Metab* 305: E161–E170, 2013.
23. **Ludwig MG, Vanek M, Guerini D, Gasser JA, Jones CE, Junker U, Hofstetter H, Wolf RM, Seuwen K.** Proton-sensing G-protein-coupled receptors. *Nature* 425: 93–98, 2003.
24. **Parks SK, Tresguerres M, Goss GG.** Interactions between Na^+ channels and Na^+-HCO_3^- cotransporters in the freshwater fish gill MR cell: a model for transepithelial Na^+ uptake. *Am J Physiol Cell Physiol* 292: C935–C944, 2007.
25. **Pastor-Soler N, Beaulieu V, Litvin TN, Da Silva N, Chen Y, Brown D, Buck J, Levin LR, Breton S.** Bicarbonate-regulated adenylyl cyclase (sAC) is a sensor that regulates pH-dependent V-ATPase recycling. *J Biol Chem* 278: 49523–49529, 2003.
26. **Paunescu TG, Da Silva N, Russo LM, McKee M, Lu HAJ, Breton S, Brown D.** Association of soluble adenylyl cyclase with the V-ATPase in renal epithelial cells. *Am J Physiol Renal Physiol* 294: F130–F138, 2008.
27. **Paunescu TG, Ljubojevic M, Russo LM, Winter C, McLaughlin MM, Wagner CA, Breton S, Brown D.** cAMP stimulates apical V-ATPase accumulation, microvillar elongation, and proton extrusion in kidney collecting duct A-intercalated cells. *Am J Physiol Renal Physiol* 298: F643–F654, 2010.
28. **Piermarini PM, Verlander JW, Royaux IE, Evans DH.** Pendrin immunoreactivity in the gill epithelium of a euryhaline elasmobranch. *Am J Physiol Regul Integr Comp Physiol* 283: R983–R992, 2002.
29. **Ramos LS, Zippin JH, Kamenetsky M, Buck J, Levin LR.** Glucose and GLP-1 stimulate cAMP production via distinct adenylyl cyclases in INS-1E insulinoma cells. *J Gen Physiol* 132: 329–338, 2008.
30. **Roa JN, Munévar CL, Tresguerres M.** Feeding induces translocation of vacuolar proton ATPase and pendrin to the membrane of leopard shark (*Triakis semifasciata*) mitochondrion-rich gill cells. *Comp Biochem Physiol A Mol Integr Physiol* 174: 29–37, 2014.
31. **Royaux IE, Wall SM, Karniski LP, Everett LA, Suzuki K, Knepper MA, Green ED.** Pendrin, encoded by the Pendred syndrome gene, resides in the apical region of renal intercalated cells and mediates bicarbonate secretion. *Proc Natl Acad Sci USA* 98: 4221–4226, 2001.
32. **Sabolić I, Brown D, Gluck SL, Alper SL.** Regulation of AE1 anion exchanger and H^+-ATPase in rat cortex by acute metabolic acidosis and alkalosis. *Kidney Int* 51: 125–137, 1997.
33. **Sahara Y, Horie S, Fukami H, Goto-Matsumoto N, Nakanishi-Matsui M.** Functional roles of V-ATPase in the salivary gland. *J Oral Biosci* 57: 102–109, 2015.
34. **Seamon KB, Daly JW.** Forskolin: a unique diterpene activator of cyclic AMP-generating systems. *J Cyclic Nucleotide Res* 7: 201–224, 1981.
35. **Smith HW.** The absorption and excretion of water and salts by the elasmobranch fishes. *Am J Physiol* 98: 296, 1931.
36. **Strazzabosco M, Fiorotto R, Melero S, Glaser S, Francis H, Spirli C, Alpini G.** Differentially expressed adenylyl cyclase isoforms mediate secretory functions in cholangiocyte subpopulation. *Hepatology* 50: 244–252, 2009.
37. **Sun X, Yang LV, Tiegs BC, Arend LJ, McGraw DW, Penn RB, Petrovic S.** Deletion of the pH sensor GPR4 decreases renal acid excretion. *J Am Soc Nephrol* 21: 1745–1755, 2010.
38. **Tresguerres M, Buck J, Levin LR.** Physiological carbon dioxide, bicarbonate, and pH sensing. *Pflügers Arch* 460: 953–964, 2010.
39. **Tresguerres M, Katoh F, Fenton H, Jasinska E, Goss GG.** Regulation of branchial V-H^+-ATPase, Na^+/K^+-ATPase and NHE2 in response to acid and base infusions in the Pacific spiny dogfish (*Squalus acanthias*). *J Exp Biol* 208: 345–354, 2005.
40. **Tresguerres M, Katz S, Rouse GW.** How to get into bones: proton pump and carbonic anhydrase in *Osedax* boneworms. *Proc Biol Sci* 280: 20130625, 2013.
41. **Tresguerres M, Levin LR, Buck J, Grosell M.** Modulation of NaCl absorption by [HCO_3^-] in the marine teleost intestine is mediated by soluble adenylyl cyclase. *Am J Physiol Regul Integr Comp Physiol* 299: R62–R71, 2010.
42. **Tresguerres M, Levin LR, Buck J.** Intracellular cAMP signaling by soluble adenylyl cyclase. *Kidney Int* 79: 1277–1288, 2011.
43. **Tresguerres M, Parks SK, Katoh F, Goss GG.** Microtubule-dependent relocation of branchial V-H^+-ATPase to the basolateral membrane in the Pacific spiny dogfish (*Squalus acanthias*): a role in base secretion. *J Exp Biol* 209: 599–609, 2006.
44. **Tresguerres M, Parks SK, Salazar E, Levin LR, Goss GG, Buck J.** Bicarbonate-sensing soluble adenylyl cyclase is an essential sensor for acid/base homeostasis. *Proc Natl Acad Sci USA* 107: 442–447, 2010.
45. **Tresguerres M, Parks SK, Wood CM, Goss GG.** V-H^+-ATPase translocation during blood alkalosis in dogfish gills: interaction with carbonic anhydrase and involvement in the postfeeding alkaline tide. *Am J Physiol Regul Integr Comp Physiol* 292: R2012–R2019, 2007.
46. **Villanger O, Veel T, Raeder MG.** Secretin causes H^+/HCO_3^- secretion from pig pancreatic ductules by vacuolar-type H^+-adenosine triphosphatase. *Gastroenterology* 108: 850–859, 1995.
47. **Wagner CA, Finberg KE, Breton S, Marshansky V, Brown D, Geibel JP.** Renal vacuolar-ATPase. *Physiol Rev* 84: 1263–1314, 2004.
48. **Wood CM, Bucking C, Fitzpatrick J, Nadella S.** The alkaline tide goes out and the nitrogen stays in after feeding in the dogfish shark, *Squalus acanthias*. *Respir Physiol Neurobiol* 159: 163–170, 2007.
49. **Wood CM, Kajimura M, Mommsen TP, Walsh PJ.** Alkaline tide and nitrogen conservation after feeding in an elasmobranch (*Squalus acanthias*). *J Exp Biol* 208: 2693–2705, 2005.
50. **Wood CM, Schultz AG, Munger RS, Walsh PJ.** Using omeprazole to link the components of the postprandial alkaline tide in the spiny dogfish, *Squalus acanthias*. *J Exp Biol* 212: 684–692, 2009.